Proceedings of the 17th World Congress
The International Federation of Automatic Control
Seoul, Korea, July 6-11, 2008

Model-Based Fault Diagnosis of a NO_x Aftertreatment System

P. Pisu*, M. Canova, A. Soliman****

**International Center for Automotive Research, Clemson University, Clemson, SC 29634 USA (Tel: 864-881-0089; e-mail: pisup@clemson.edu).*
***Center for Automotive Research, The Ohio State University, Columbus, OH 43212 USA (e-mail: canova.1@osu.edu, soliman.1@osu.edu)*

Abstract: The Lean NO_x Trap (LNT) is an aftertreatment device used to attain a reduction in nitrogen oxide emissions for Diesel and lean burn engines. The LNT is typically used as a storage device, capturing NO_x during lean engine operation. The trap can be regenerated by controlling the exhaust air-fuel ratio to create a rich gas mixture. Under rich conditions, the stored NO_x is released and catalytically converted. This way, tailpipe emissions can be significantly reduced by properly modulating the lean (storage) and rich (regeneration) periods. To maintain the LNT operate with high conversion efficiency, an optimized control of the regeneration scheduling is required. In addition, LNT systems require fault diagnostic schemes to detect and isolate faults, typically related to sulfur and thermal damages. This paper deals with the design and validation through simulation of a model-based fault diagnosis scheme for a LNT system. The mathematical model of the subsystem, based on the physics of the processes involved, consist of time-varying nonlinear ODEs. The proposed diagnostic approach is based on the generation of residuals using system models and through comparison of the predicted and measured value of selected variables, including the AFR, catalyst output temperature and the NO_x concentration at the output of the LNT. The paper focuses on detection and isolation of controller faults and LNT parametric faults related to sulfur and thermal damage. The model utilized in the diagnostic scheme, which includes sulfur poisoning and thermal deactivation processes, has been experimentally validated from data collected on a Diesel LNT system and integrated with a quasi-steady engine and vehicle simulator to estimate tailpipe emissions during standard driving cycles.

1. INTRODUCTION

Nitrogen Oxides (NO_x) are one of the primary pollutants in Diesel and gasoline lean burn engines. Their formation is particularly difficult to control, due to the lean, oxygen-rich exhaust conditions that hinder the chemical reduction reactions of NO and NO_2 to N_2. For this reason, the most viable solutions to attain a reduction in NO_x emissions involve the use of aftertreatment technologies. Currently, various systems are being studied and some of them are already implemented in production automobiles, as well as light duty and heavy duty trucks (Charlton, 2005).

Lean NO_x Traps (LNTs) offer an attractive solution for passenger cars, and light-duty trucks powered by lean burn gasoline and Diesel engines. During lean engine operations, these catalysts operate as storage devices, isolating the NO_x from the exhaust gas and storing it as Barium Nitrate ($BaNO_3$). The LNT can be regenerated by periodically producing rich, reducing exhaust gas that releases and reduces the stored NO_x (Brandt *et al.,* 2000, Larsson *et al.*, 1999). However, the periodic regeneration is typically accomplished by injecting additional fuel, which penalizes the fuel consumption and increases CO, hydrocarbons and soot emissions.

For this reason, controlling the LNT regeneration frequency and operations to meet emission standards and fuel economy targets is a critical challenge. The LNT performance during the storage and regeneration phases is strongly affected by several operating parameters, such as air/fuel ratio, gas composition, temperature, and space velocity.

In addition, LNT catalysts are subject to failures, typically related to aging and sulphur poisoning, which can compromise the storage performance of the catalyst if not properly monitored and compensated for. Since EPA requires fault diagnosis schemes to detect failure and diagnose faults to meet OBD II standards (Baltusis, 2004), the LNT control problem implies the design and application of fault diagnosis techniques.

In order to address applications related to the control and diagnostics, several control-oriented models of LNT systems have been developed (Hepburn *et al.*, 1996, Larsson *et al.*, 1999, Kim *et al.,* 2003, Van Nieuwstadt and Yanakiev, 2004). However, most of the approaches proposed present limitations in the capability of accurately characterizing the dynamics of the LNT system, for example, not accounting for phenomena such as oxygen storage and release dynamics or for temperature dynamics. In addition, the degradation of LNT storage efficiency due to aging, sulphur poisoning or thermal deactivation is often not considered. Such features become a main concern when the objective of the study is to design adaptive control strategies or to explore model-based fault diagnosis.

This paper presents a model-based fault diagnosis scheme for a LNT, focused on the detection and isolation of controller faults and system faults related to sulfur poisoning and thermal damage. The fault diagnosis scheme is applied to a mathematical model of the LNT system, in the form of time-varying nonlinear ODEs. The model, validated on experimental data, is coupled with a quasi-steady engine emission model and a Diesel Oxidation Catalyst (DOC) model to simulate the behavior of a Diesel NO_x aftertreatment system in standard driving cycles.

The proposed diagnostic approach is based on the generation of residuals using system models and through comparison of the predicted and measured value of selected variables, including the AFR, catalyst output temperature and the NO_x concentration at the output of the LNT.

2. LEAN NO_x TRAP MODELING METHODOLOGY

The fault diagnosis study is based on a model of a LNT catalyst that captures the most relevant physical and chemical phenomena which characterize the system dynamics, while maintaining real-time computational capability. The model is based on a grey-box approach, where the basic conservation principles are applied (Canova, 2006), together with a phenomenological characterization of the reaction mechanisms during the storage and release phases (Kim *et al.,* 2003, Van Nieuwstadt and Yanakiev, 2004).

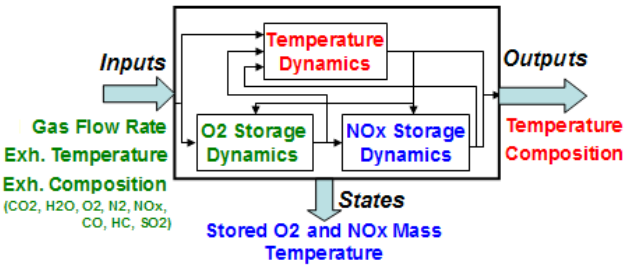

Fig. 1. Structure of the LNT model.

As shown in Figure 1, the LNT system dynamics results from the interaction of three subsystems, namely the oxygen storage dynamics, the NO_x storage dynamics and the temperature dynamics.

The inputs are the exhaust gas mass flow rate and temperature, together with the composition of the feed gas, for which eight species are considered (CO_2, H_2O, O_2, N_2, NO, CO, C_nH_m, SO_2).

The outputs of the model are the outlet gas temperature (assumed equal to the catalyst brick temperature) as well as the outlet mixture composition. The resulting air/fuel ratio is calculated from the concentrations of CO_2, H_2O, O_2, CO and hydrocarbons (Heywood, 1988).

The model equations, thoroughly described in (Canova *et al.,* 2007), will be briefly presented to illustrate the application to model-based fault diagnosis.

2.1 Oxygen Storage/Release Dynamics

Oxygen storage and release are relevant phenomena that affect the air/fuel ratio of the mixture and, ultimately, the NO_x concentration in the catalyst. The model is based on the application of the continuity equation to the oxygen stored (in solid state) and to the oxygen present in the exhaust stream (gas phase). This allows one to write the state equation (which characterizes the storage/release dynamics) and output equation (which yields the outlet oxygen mass flow rate), as in the following:

$$\frac{dM_{O_2}}{dt} = r_{O_2,stor} - r_{O_2,rel} \tag{1}$$

$$\dot{m}_{O_2,out} = \dot{m}_{O_2,in} - r_{O_2,stor} + r_{O_2,rel} \tag{2}$$

The mass of stored oxygen, M_{O2}, is equal to the product between the oxygen capacity C_{O2} and the fill ratio x, normalized in the [0,1] interval. The fill ratio is defined as the current mass stored divided by the maximum storage capacity at the current conditions. The storage capacity is a function of catalyst temperature:

$$C_{O_2} = C_m \exp\left[-\left(\frac{T - T_m}{T_s}\right)^2\right] \tag{3}$$

where C_m, T_m and T_s are model parameters experimentally identified.

Based on a phenomenological observations (Brandt *et al.,* 2000), the oxygen storage and release rate, $r_{O2,stor}$ and $r_{O2,rel}$, have a nonlinear dependence on the fill ratio and are proportional to the inlet mass flow rates of oxygen and reductants, respectively:

$$\begin{aligned} r_{O_2,stor} &= k_{st}\left(\frac{1-e^{\alpha x}}{e^{\alpha}-1}+1\right)\dot{m}_{O_2,in} \\ r_{O_2,rel} &= k_{rel}\left(\frac{e^{-\beta x}-1}{e^{-\beta}-1}\right)\left(\dot{m}_{CO}+\dot{m}_{HC}\right)_{in} \end{aligned} \tag{4}$$

where k_{st} and k_{rel} are empirical constants and the multipliers α and β are considered linear function of the catalyst temperature T. The formulation described in (4) assumes that the exhaust gas mixture does not contain any CO or HC during lean operations (storage). In a lean-burn engine aftertreatment system, this is typically ensured by an oxidation catalyst upstream the LNT.

From Equation (2), the oxygen flow rate released during the regeneration phase combines immediately with the available reductants (CO and hydrocarbons) and the resulting mixture composition is calculated with mass balances based on the following reactions:

$$\begin{aligned} CO + \frac{1}{2}O_2 &\rightarrow CO_2 \\ C_nH_m + \left(n + \frac{m}{4}\right)O_2 &\rightarrow nCO_2 + \frac{m}{2}H_2O \end{aligned} \tag{5}$$

It is important to observe that the model assumes the O_2 storage and release phenomena prevailing over the NO_x ones. In particular, if storage sites are available in the catalyst and the engine exhaust gas is lean, the oxygen will be stored before the NO_x. Conversely, if oxygen is stored in the LNT and the feed gas is rich, the reductants will release and combine with the oxygen first.

2.2 NO_x Storage/Release Dynamics

The dynamics associated with the NO_x adsorption and release are described with a similar approach, namely, by defining a state equation, which yields the mass of NO_x stored in the LNT, and an output equation representing the NO_x mass flow rate balance in gas phase. The equations are characterized by parameters that depend on inputs and states such as the temperature, inlet mass flow rate and catalyst fill ratio:

$$\frac{dM_{NO_x}}{dt} = C_{NO_x}\frac{dx}{dt} = r_{NO_x,stor} - r_{NO_x,rel} \tag{6}$$

$$\dot{m}_{NO_x,out} = \dot{m}_{NO_x,in} - r_{NO_x,stor} + r_{NO_x,rel} \tag{7}$$

Similarly to Equation (3), the storage capacity is empirically found dependent on the catalyst temperature. In addition, a linear relation with the inlet gas mass flow rate is included to improve the accuracy:

$$C_{NO_x} = C_m\left(\kappa_1\dot{m}_{gas} + \kappa_0\right)\exp\left[-\left(\frac{T-T_m}{T_s}\right)^2\right] \tag{8}$$

The storage rate is based on the following simplified reactions (Van Nieuwstadt and Yanakiev, 2004):

$$\begin{aligned} &NO + \frac{1}{2}O_2 \rightarrow NO_2 \\ &2NO_2 + BaCO_3 + \frac{1}{2}O_2 \rightarrow Ba(NO_3)_2 + CO_2 \end{aligned} \tag{9}$$

Since the storage reactions consume oxygen, it is important to account for the interactions with the O_2 storage dynamics. This can be done by adding an efficiency term in the storage model equation:

$$r_{NO_x,stor} = k_{st}\eta_c\left(\frac{1-e^{\gamma x}}{e^{\gamma}-1}+1\right)\dot{m}_{NO_x,in} \tag{10}$$

The multiplier γ depends linearly on the catalyst temperature. The efficiency term η_c accounts for the oxygen available to promote the NO_x storage reactions:

$$\eta_c = \frac{e^{-\delta z}-1}{e^{\delta}-1} \tag{11}$$

where the multiplier δ is a linear function of the temperature and z represents the ratio between the mass flow rates of O_2 and NO_x, normalized by the corresponding stoichiometric value calculated from (9).

The trap regeneration process occurs in two phases. First, the stored NO_x are released from the trap in presence of rich exhaust conditions. The barium nitrate becomes unstable releasing NO_2 and the surface site converting to BaO, which combines with CO_2 to form $BaCO_3$, completing the regeneration of the trap. The reaction mechanisms can be summarized by the following simplified reactions:

$$\begin{aligned} &Ba(NO_3)_2 \rightarrow BaO + NO_2 + \frac{1}{2}O_2 \\ &BaO + CO_2 \rightarrow BaCO_3 \end{aligned} \tag{12}$$

Based on previous results (Van Nieuwstadt and Yanakiev, 2004), the release rate is given by the following expression:

$$r_{NO_x,rel} = k_{rel}\left(\frac{e^{-\phi x}-1}{e^{-\phi}-1}\right)\left(\dot{m}_{CO} + \dot{m}_{HC}\right)^*_{in} \tag{13}$$

where the term $\left(\dot{m}_{CO} + \dot{m}_{HC}\right)^*_{in}$ denotes the mass flow rate of reductants available after the combination with the oxygen released during regeneration. The released NO_2 is then catalytically converted to N_2 by the available reductants. The process can be simplified to three basic reactions:

$$\begin{aligned} &NO_2 \rightarrow NO + \frac{1}{2}O_2 \\ &NO + CO \rightarrow CO_2 + \frac{1}{2}N_2 \\ &\left(2n+\frac{m}{2}\right)NO + C_nH_m \rightarrow nCO_2 + \frac{m}{2}H_2O + \\ &\qquad + \left(n+\frac{m}{4}\right)N_2 \end{aligned} \tag{14}$$

The conversion process depends on the catalyst temperature, fill ratio and concentration of CO and hydrocarbons available in the mixture. Therefore, the rate of conversion to N_2 can be defined as:

$$r_{NO_x,conv} = k_{conv}\eta_{conv}r_{NO_x,rel} \tag{15}$$

where the conversion efficiency is a complex function that includes the effects of the mentioned variables:

$$\eta_{conv} = \left(\frac{e^{\lambda x}-e^{\lambda}}{1-e^{\lambda}}\right)\left(\frac{e^{-\sigma u}-1}{e^{-\sigma}-1}\right) \tag{16}$$

where λ is a linear function of the catalyst temperature and u represent the mass of equivalent reductant ($CO+C_nH_m$) that is required to convert the released NO_x, normalized to the corresponding stoichiometric value, which can be obtained from the reactions (14). Elementary mass balances are then used to calculate the concentration at the catalyst outlet. The parameters in (13), (15) and (16) have been identified with experimental data during storage and regeneration cycles at different engine operating conditions using data from previous work (Choi *et al.,* 2005).

2.3 Catalyst Temperature Dynamics

The LNT temperature can be estimated with an energy balance for an open thermodynamic system, considering the catalyst brick temperature equal to the temperature of the gas in the system. This simplification can be justified by the small diameter of the passages inside the catalyst, which reduces the average gas velocity. With this assumption, the energy balance yields:

$$\frac{dT}{dt} = \frac{1}{M_{cat} c_{cat}} \left[\dot{m}_{gas} c_p \left(T_{in} - T \right) + \dot{Q}_{reac} - \dot{Q}_{ht} \right] \tag{17}$$

where $M_{cat}c_{cat}$ denotes the catalyst thermal capacity, c_p is the specific heat of the feed gas and Q_{ht} is relative to the heat losses due to convection. The term Q_{reac} is calculated from the reaction enthalpy associated to the release and conversion reactions of the stored O_2 and NO_x (Choi *et al.*, 2005).

3. LNT FAULTS MODELING APPROACH

The possibility of characterizing system failure modes is an important feature of the LNT model, allowing for implementing fault detection and isolation algorithms. The model considers, in a phenomenological way, effects on storage and release dynamics of sulphur poisoning and thermal deactivation. The model is based on results from previous experimental studies (Choi *et al.,* 2005).

Modeling the effects caused by sulphur poisoning on a LNT is important in case of Diesel engine aftertreatment, since Diesel fuel for automotive applications contains sulphur concentrations that may reach 15ppm in mass permitted by the Tier 2 US standard. During the combustion, the sulphur combines with the available oxygen creating sulphur dioxide, which poisons the catalytic converters by occupying the available storage sites. The process can be simplified by considering the following reactions:

$$\begin{aligned} &SO_2 + \frac{1}{2} O_2 \leftrightarrow SO_3 \\ &BaCO_3 + SO_3 \leftrightarrow BaSO_4 + CO_2 \end{aligned} \tag{18}$$

The sulphur storage and release processes are strongly affected by temperature. In particular, $BaSO_4$ is stable under lean conditions; the decomposition is possible only at temperatures above 700°C (depending on the catalyst composition) and under rich conditions. These effects can be modeled by adopting a grey-box approach, similar to the oxygen storage dynamics. In particular, the following relations characterize the mass of stored SO_2, as well as the storage and release rate:

$$\frac{dM_{SO_2}}{dt} = C \frac{dx}{dt} = r_{SO_2,stor} - r_{SO_2,rel} \tag{19}$$

$$r_{SO_2,stor} = k_{st} \left(\frac{1 - e^{\xi x}}{e^{\xi} - 1} + 1 \right) \dot{m}_{SO_2,in} \tag{20}$$

$$r_{SO_2,rel} = k_{rel} f_{rel}(T) \left(\frac{e^{-\zeta x} - 1}{e^{-\zeta} - 1} \right) \left(\dot{m}_{CO} + \dot{m}_{HC} \right)_{in} \tag{21}$$

The expression for SO_2 release rate is characterized by a temperature activation function:

$$f_{rel}(T) = \frac{1}{1 + e^{-k\left(T - T_{activation}\right)}} \tag{22}$$

The sulphur storage and release reactions are considered predominant over the O_2 and NO_x. The trap capacity C, is evaluated as a function of temperature as in Equation (3) and the remaining parameters can be determined from experimental data.

The mass of stored SO_2 is then subtracted from the O_2 and NO_x capacities to model the deactivation of storage sites consequent to the trap poisoning. In addition, experimental studies (Choi *et al.,* 2005) show that the cumulative LNT storage efficiency, defined as the ratio between the integrated NO_x stored mass flow rate expressed by (10) and the integrated inlet NO_x mass flow rate, decreases almost linearly with increasing levels of sulphur poisoning. This effect, which is a consequence of the reduction of active storage sites, can be captured by introducing a correction to the NO_x storage rate, depending on the ratio between the mass of stored sulphur and the trap capacity:

$$r_{NO_x,stor} = k_{st} \eta_c f\left(\frac{M_{SO_2}}{C_m} \right) \left(\frac{1 - e^{\gamma x}}{e^{\gamma} - 1} + 1 \right) \dot{m}_{NO_x,in} \tag{23}$$

Unlike sulphur poisoning, thermal damage is arduous to model, as very few specific studies are available in this field. For this reason, a physically-based methodology can not be considered, forcing to adopt a simple phenomenological approach. According to (Choi *et al.,* 2005), thermal damaging effects occur as a consequence of very high LNT temperatures, which rapidly cause the deactivation of the active storage sites in the catalyst.

From a modeling perspective, the variables mostly affected by the phenomenon are the O_2, NO_x and SO_2 storage capacities. Therefore, thermal damage can be approximately accounted for by defining a correction term, which linearly depends on the brick temperature value and the duration of the thermal stress. In case of the O_2 storage capacity, the new expression becomes:

$$C_{O_2} = C_m \exp\left[-\left(\frac{T - T_m}{T_s} \right)^2 \right] f_{dam}(\Delta T, t) \tag{24}$$

where the correction term is given by:

$$f_{dam}(\Delta T, t) = \begin{cases} 1, & T < T_{dam} \\ 1 - k_{dam} \int_t (T - T_{dam}) dt, & T \geq T_{dam} \end{cases} \tag{25}$$

The temperature threshold for thermal damage depends on the trap and catalyst composition, and is generally around 750°C under lean conditions.

3. LNT MODEL VALIDATION

As described in (Canova *et al.,* 2007), the LNT model was validated with experimental data obtained on a 4 cylinder Diesel engine. The tests made were relative to steady-state engine conditions, and consisting of storage and regeneration cycles with an increasing storage time and fixed regeneration period of 20s. The engine was maintained at constant speed and torque to provide lean exhaust with high NO_x content, while the rich conditions for regeneration were provided by partially diverting the gas flow from the LNT with a bypass valve and injecting CO in the stream. Figure 2 shows the values of the main model inputs during a portion of the experimental test.

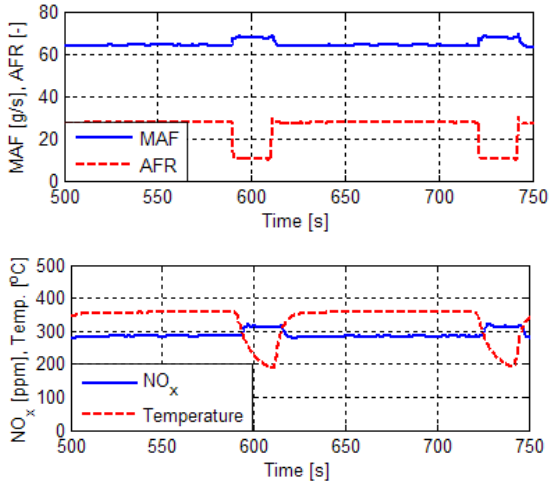

Fig. 3. . MAF, AFR (top) NO_x concentration and temperature (bottom) at the LNT inlet.

In Figure 3, the estimated NO_x concentration at the catalyst outlet is compared to the experimental data, showing good agreement.

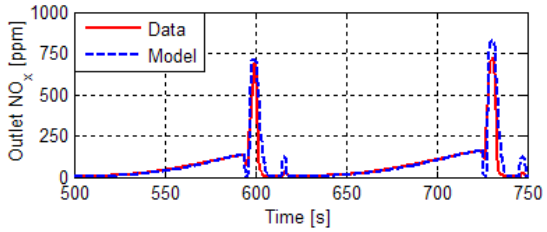

Fig. 3. Comparison of outlet NOx emissions.

The model is capable of capturing the most relevant details of the LNT system dynamics, including the characteristic NO_x slip during the initial part of the regeneration phase, caused by the lack of reductants to combine with the released NO_x due to the reactions with the released oxygen.

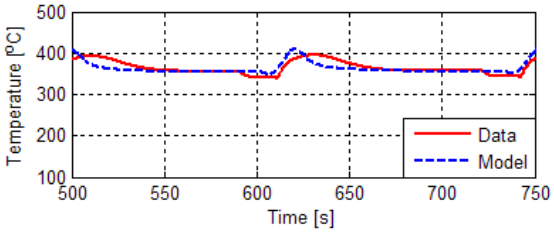

Fig. 4. Comparison of catalyst outlet temperature.

Figure 4 compares the estimated LNT temperature with the value acquired with a thermocouple at the catalyst outlet. Despite the fair accuracy in the steady-state temperature values (during storage phase), the results show a sub-optimal agreement during the regeneration phase. The reason has to be found in the spatial distribution of temperatures and concentrations inside the catalyst, which could be captured by adopting spatially resolved calculations or lumped parameter models, if a higher accuracy is required.

5. MODEL OF A NO_x AFTERTREATMENT SYSTEM

As a final stage of development, a model of a Diesel NO_x aftertreatment system was created by combining the LNT model with a quasi-steady engine emissions model (derived from the interpolation of the steady-state engine emission data) and a model of a Diesel oxidation catalyst. Simple models for oxygen, NO_x and temperature sensors were also developed. A schematic of the aftertreatment system layout is shown in Figure 5.

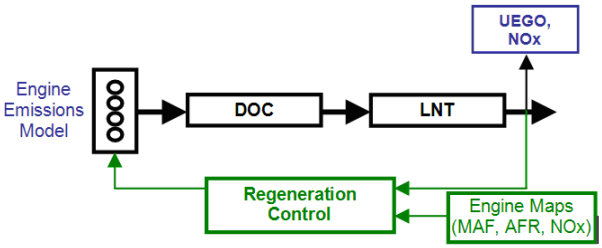

Fig. 5. Diesel NOx aftertreatment system model.

A regeneration controller was designed to schedule the LNT regeneration events and to provide closed-loop control of the engine Air/Fuel Ratio (AFR) during the rich phase.

The controller requires the engine air mass flow rate, AFR, NOx concentration and gas temperature at the exhaust. These signals are obtained from the steady-state engine calibration maps (as a function of engine speed and torque). In addition, the controller has a feedback on the NO_x concentration and AFR at the LNT outlet. These signals can be acquired using solid-state NO_x and UEGO sensors. For diagnostic purposes, the gas temperature at the LNT outlet is also required.

The controller triggers the regeneration when the cumulative NO_x storage efficiency of the catalyst drops below a threshold value (set to 0.9):

$$\eta_{stor} = 1 - \frac{\int_{storage} \dot{m}_{NO_x,out}\, dt}{\int_{storage} \dot{m}_{NO_x,in}\, dt} \tag{26}$$

where the integral terms of Equation (26) are calculated with respect to the storage phase.

The duration of the rich phase is controlled by the air/fuel ratio at the LNT outlet, which remains close to its

stoichiometric value until the stored O_2 and NO_x are completely released from the trap. The control strategy attempts to prevent the reductant slip, which could compromise the CO and HC emissions, and also impact fuel consumption. During the regeneration phase, the engine air/fuel ratio is modulated by a feedback PI control based on the outlet NO_x concentration. An additional feed-forward term ensures a faster response during the initial transient of the regeneration phase.

6. FAULT DIAGNOSIS SCHEME

This section describes the design of a diagnostic scheme for thermal damage and sulfur poisoning fault conditions, by using the LNT model described in the previous section.

The fault diagnosis scheme is based on a parity equation approach, comparing the behavior of the system with the behavior of the aftertreatment model to produce residuals that contain useful fault information (Kimmich *et al.,* 2005, Pisu *et al.*, 2003). The scheme is based on the following assumptions:

- Residuals are considered only during the storage phase (lean operation);
- The flow rate $\dot{m}_{NO_x,out}$ can be calculated from the NO_x sensor with a sufficient precision;
- The regeneration control is saturated or is not robust enough to reject the faults;
- The sensors are fault free;
- The temperature in and out of the LNT is measured.

Figure 6 shows a block diagram of the diagnostic scheme.

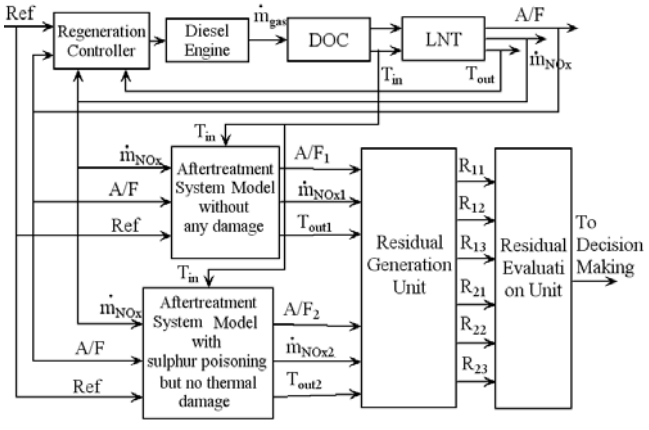

Fig. 6. Model-based diagnostic scheme.

Fault detection can be performed through a simple comparison of the AFR, NO_x and temperature measurements from the system with the value calculated from the models. Six residuals, defined in (28), are considered for fault detection and isolation:

$$\begin{aligned} R_{11} &= AFR - (AFR)_1 & R_{12} &= \int_{storage} \left(\dot{m}_{NO_x} - \dot{m}_{NO_x,1}\right) dt \\ R_{13} &= T_{out} - T_{out,1} & R_{21} &= AFR - (AFR)_2 \\ R_{22} &= \int_{storage} \left(\dot{m}_{NO_x} - \dot{m}_{NO_x,2}\right) dt & R_{23} &= T_{out} - T_{out,2} \end{aligned} \quad (28)$$

Since the residuals are never equal to zero even in absence of faults due to noise and model uncertainties, threshold levels are set that have to be exceeded before a residual is considered non-zero. The thresholds are derived statistically to minimize false alarms by calculating the normal deviations of the estimates from the measured variables during several tests under no fault conditions. Under the assumption of single fault occurrence, and observing the residual generation structure, the following fault isolation logic can be derived as listed in Table 1.

Table 1. Error signature for aftertreatment system faults.

Fault	R_{11}	R_{12}	R_{13}	R_{21}	R_{22}	R_{23}
None	0	0	0	0	0	0
Controller	1	1	1	1	1	1
SO_2 poisoning	0	1	x	0	0	0
Thermal damage	0	x	1	0	x	1

It is important to notice that, if the regeneration controller is robust and therefore rejects the systems faults, the diagnostic model needs to be modified by considering in the residual generation the measurement of AFR and NO_x at the input of the LNT instead of the output.

7. SIMULATION RESULTS

In order to test the effectiveness of the FDI scheme, a number of simulations were run, in which various faults were induced in the aftertreatment system and the data was used to generate residuals as described above. The results presented are related to tests for thermal damage fault and sulfur poisoning. All the tests are performed with the engine operating at constant speed and torque.

A thermal deactivation fault was introduced in the LNT system after 5 minutes of simulation, by increasing the reaction heat Q_{reac} (in Equation 17), during one regeneration.

This modification simulates the effects of a leak in the exhaust system, causing the introduction of air in the exhaust gas. If extra oxygen is present in the LNT feed gas during regeneration, it will immediately combine with the available reductants, favorite by the reactor catalytic material. This will cause a surge in the catalyst temperature, captured by the LNT outlet sensors.

As shown in Figure 7, the FDI scheme correctly detects the thermal damage fault, as the residuals R31 and R32 (based on the outlet temperature), exceed the pre-set threshold. The residuals R12 and R22, based on the outlet NO_x, show a delay in the fault detection, as thermal damage does not immediately affect the outlet NO_x flow rate. Conversely, the

residuals R11 and R21, not shown in figure, never cross the corresponding threshold during the presence of the fault. Therefore, the residual vector during the faulty portion of the test assumes the value **R**=[0 x 1 0 x 1], indicating the presence of thermal deactivation fault.

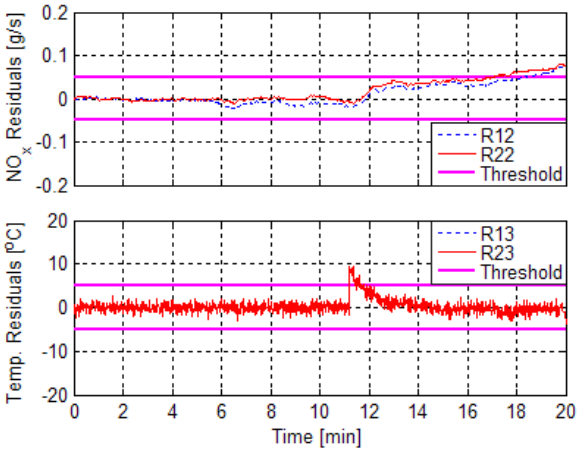

Fig. 7. Residuals for thermal damage fault diagnosis

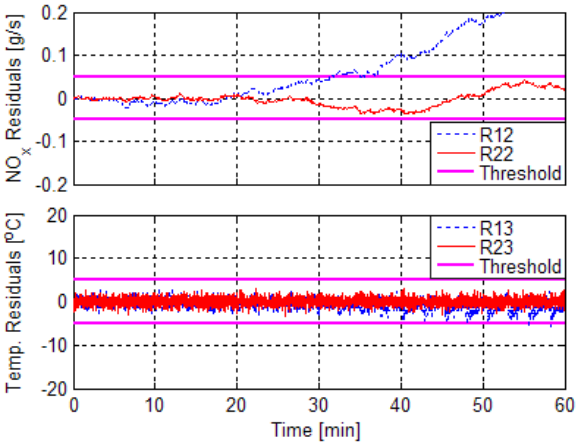

Fig. 8. Residuals for sulfur poisoning fault diagnosis

Figure 8 shows the residuals values when a sulfur poisoning fault is introduced after 10 minutes of simulation, by injecting a constant SO_2 concentration of 100ppm in the exhaust gas. In this case, only the residuals R12 exceeds the correspondent thresholds, while the behavior of the residuals R22 and R23 is indifferent to the fault isolation process. Moreover, the residual R13 requires a longer time to detect a poisoning fault in the system. For these reasons, the residual vector becomes **R**=[0 1 x 0 0 0], as denoted in Table 1. It is worth observing that the sulfur poisoning detection occurs after over 20 minutes from the fault injection, especially considering the high SO_2 concentration injected. This demonstrates the difficulty of detecting sulfur poisoning, which is a process that typically occurs over a long time range. Even though the poisoning detection could be anticipated by tightening the threshold values, this will increase the risk of false positive detections.

8. CONCLUSION

The paper presents a model-based diagnostic approach applied to a Diesel engines NO_x aftertreatment system for the detection and isolation of sulfur poisoning and thermal damage. The model used in the study, based on the physics of the processes involved, captures the relevant steady-state and transient phenomena, including oxygen and NO_x storage and release dynamics, as well as temperature dynamics. A phenomenological characterization of sulfur poisoning and thermal damage processes is included. The model has been experimentally validated on a LNT system and further extended to characterize a complete Diesel engine aftertreatment system (inclusive of regeneration control).

Using this tool, a fault diagnosis scheme was designed to detect the LNT system faults. The approach is based on the generation of residuals from the comparison of the predicted and measured value of selected variables.

The proposed scheme shows to be effective in isolating both sulfur poisoning and thermal damage fault within a reasonable amount of time from the occurrence of the fault. On-going research is addressing validation of the proposed diagnostic scheme with an experimental setup.

REFERENCES

Baltusis, P., (2004). On Board Vehicle Diagnostics, *SAE Technical Paper 2004-21-0009*.

Charlton, S., (2004). Developing Diesel Engines to Meet Ultra-Low Emission Standards, *SAE Technical Paper 2005-01-3628, 2005.*

Brandt, E., Wang Y. and Grizzle, J., (2000). Dynamic Modeling of a Three-Way Catalyst for SI Engine Exhaust Emission Control, *IEEE Transactions on Control System Technology*, 8(5).

Canova, M., (2006). *Fluid Systems Dynamics Modeling for Control: Internal Combustion Engines Case Studies*, Ph.D. Dissertation, University of Parma.

Canova, M., Midlam-Mohler, S., Soliman, A., Guezennec, Y. and Rizzoni, G., (2007). Control-Oriented Modeling of NOx Aftertreatment Systems, *8th International Conference on Engines for Automobile, Capri, Italy.*

Choi, I., Zou, Z., Midlam-Mohler, S., Soliman, A. and Rizzoni, G., (2005). Modeling and Diagnostics of NO_x Aftertreatment System. *Proceedings of FISITA World Automotive Congress*.

Hepburn, J., Thanasiu, E., Dobson, E. and Watkins, W., (1996) Experimental and Modeling Investigations of NO_x Trap Performance, *SAE Technical Paper 962051*.

Heywood, J., (1988). *Internal Combustion Engines Fundamentals*, McGraw-Hill.

Kimmich, F., Schwarte, A. and Isermann, R., (2005). Fault Detection for Modern Diesel Engines Using Signal- and Process Model-Based Methods, *Control Engineering Practice*, 13(2005): pp. 189-203.

Kim, Y., Sun, J., Kolmanovsky, I. and Koncsol, J., (2003). A Phenomenological Control Oriented Lean NO_x Trap Model, *SAE Technical Paper 2003-01-1164*.

Larsson, M., Andersson, L., Fast, O., Litorell, M. and Makuie, R., (1999). NO_x Trap Control by Physically Based Model, *SAE Technical Paper 1999-01-3503*.

Pisu, P., Soliman, A. and Rizzoni, G., (2003). Vehicle Chassis Monitoring System, *Control Engineering Practice*, 11(3): pp. 345-354.

Van Nieuwstadt, M., and Yanakiev, O. (2004). A Diesel Lean NO_x Trap Model for Control Strategy Verification, *SAE Technical Paper 2004-01-0526*.